Research Journal of Applied Sciences, Engineering and Technology 7(17): 3499-3513, 2014
DOI:10.19026/rjaset.7.702
ISSN: 2040-7459; e-ISSN: 2040-7467

Submitted: October 19, 2013 Accepted: October 28, 2013 Published: May 05, 2014

Research Article

Retinopathy of Prematurity Vessel and Ridge Parameters Measurement by Unsupervised Algorithm

[1]S. Prabakar, [2]K. Porkumaran, [3]Parag K. Shah and [3]V. Narendran
[1]Department of Electronics and Communication Engineering, Kathir College of Engineering, Coimbatore-641062, India
[2]N.G.P. Institute of Technology, Coimbatore-641048, India
[3]Department of Paediatric Retina and Ocular Oncology, Aravind Eye Hospitals, Coimbatore, India

Abstract: The Retinopathy of Prematurity (ROP) is an ocular pathological disorder of the retinal blood vessels in premature infants and low birth weight infants. It is essential that those caring for premature infants should know who is at risk of ROP and their severity stage. It is also important that when screening must begin and how often these infants need to be examined otherwise the progression lead most severe stage and can cause blindness. The contrast stretching method has been utilized to enhance the ROP color image. Then an automatic method Isotropic Un-decimated Wavelet Transform (IUWT) has been proposed to extract the abnormal retinal blood vessel and measure its width and tortuosity. The ridge formation of this pathological disorder has also been obtained by the IUWT. The quantitative measurements of mean diameter, standard deviation, tortuosity, length of retinal blood vessel and ridge have been considered and computed the exact severity stage of ROP. The effectiveness of the proposed method has been verified through machine vision techniques and the results obtained are encouraged by experts. Automatic ROP screening system comprises several advantages, like a substantial time reduction of ophthalmologists in diagnosis, a non ophthalmologist can provide stage of ROP, improving the sensitivity of the test and a better accuracy in diagnosis.

Keywords: Premature infants, retinal vessel, retinopathy of prematurity, ROP screening, un-decimated wavelet transform

INTRODUCTION

Image processing, analysis and computer vision techniques are widely used today in all fields of medical sciences and especially to modern ophthalmology, as it is heavily dependent as visually oriented signs. The Retinopathy of Prematurity (ROP) is a pathological disorder of the retinal blood vessels which frequently develops in premature infants. It is characterized by blood vessel width, tortuosity of the vessels and ridge formation in various zones in the retinal area. The optic disk, macula and fovea are the important landmarks for zone selection and represent the severity level of ROP disease in premature infants. This study presents a new, fast, fully automatic retinal vessel segmentation, tortuosity, ridge and vessel width measurement algorithms have been utilized for screening the ROP stages (Parag *et al*., 2011).

Retinopathy of Prematurity (ROP) is an ocular disease of premature infants and it can cause blindness at high risk pre-threshold stages (Early Treatment of Retinopathy of Prematurity Cooperative Group (ETROP), 2003). It affects immature vasculature in the eyes of premature babies (Wittchow, 2003; Mounir *et al*., 2008). It can be mild with no visual defects, or it may become aggressive with new blood vessel formation (neovascularization) and progress to retinal detachment and blindness (International Committee for the Classification of Retinopathy of Prematurity (International Committee for the Classification of Retinopathy of Prematurity, 2005). As smaller and younger babies are surviving, the incidence of ROP has increased (Gwenole *et al*., 2008; Lam and Hong, 2008). All babies who less than 1800 g birth weight or younger than 32 weeks gestational age at birth are at risk of developing ROP.

In any Neonatal Intensive Care Unit (NICU), the timing of the first evaluation must be based on the gestational age at birth:

- If the baby is born at 23-24 weeks' gestational age, the first eye examination should be performed at 27-28 weeks gestational age.

Corresponding Author: S. Prabakar, Department of Electronics and Communication Engineering, Kathir College of Engineering, Coimbatore-641062, India

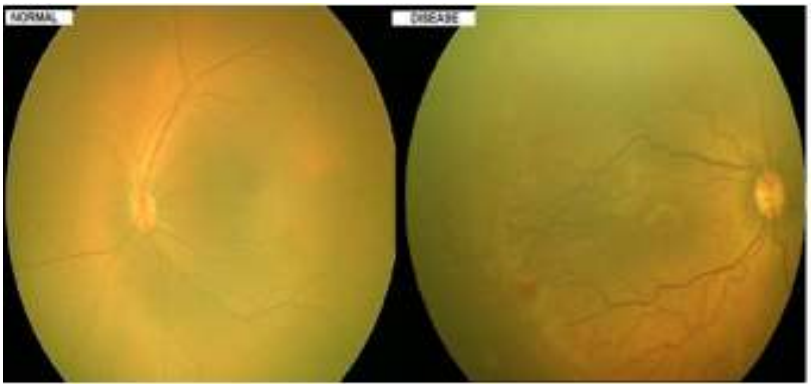

Fig. 1: Normal and diseased retinal blood vessels image of premature babies

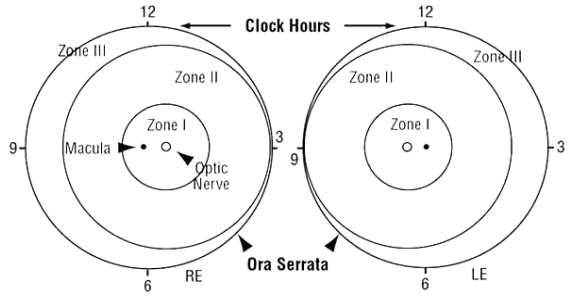

Fig. 2: Zone 1 is the most posterior retina that contains the optic nerve and the macula (zone of acute vision); zone 2 is the intermediate zone where blood vessels often stop in ROP; zone 3 is the peripheral zone of the retina, where vessels are absent in ROP, but present in normal eyes

- If the baby is born at or beyond 25-28 weeks' gestational age, the first examination should occur at the fourth to fifth week of life.
- Beyond 29 weeks, the first eye examination should probably occur by fourth week life time of baby.

It is essential that those caring for premature infants know who is at risk of retinopathy of prematurity, when screening must begin and how often these infants need to be examined. It is also important to know when to treat those infants who develop severe retinopathy of prematurity and what long term follow-up is needed to manage other complications of retinopathy of prematurity (Shankar, 1986; Conor *et al*., 2002). The discrimination between normal retinal vessels and diseased vessels plays a vital role to detect the ROP as shown in Fig. 1. The ROP occurs when abnormal blood vessels develop at the edge of normal retinal blood vessel. The ophthalmologists who are trained in ROP have to study and analyze the Retcam images.

Classification of ROP: Blood vessel development in the retina occurs from the optic nerve out towards the periphery, that is, from the back of the eye towards the front. The location of the disease is referred by the ICROP (International Classification of Retinopathy of Prematurity) classification and is a measure of how far this normal progression of blood vessel development has progressed before the disease takes over (Mounir *et al*., 2008). Generally Zone II disease is more severe than Zone III disease and Zone I disease is the most dangerous of all since progression to extensive scar tissue formation and total retinal detachment is most likely in this location.

From the "flattened" retina shown in Fig. 2, we can see that:

- Zone I is a small area around the optic nerve and macula at the very back of the eye.
- Zone II extends from the edge of Zone I to the front of the retina on the nasal side of the eye (i.e., nose side) and part way to the front of the retina on the temporal side of the eye (i.e., temple side, or side of the head).
- Zone III is the remaining crescent of retina in front of Zone II on the temporal side of the eye.

Think of the eye as in time sections of a twelve hour clock to classify the stages of ROP. The extent of ROP is defined by how many clock hours of the eye's circumference are diseased. The numbers around the "flattened" retina in the Fig. 2 shows the hours of the clock for each eye. For example, 3 o'clock is to the right, which is on the nasal side for the right eye and temporal side for the left eye (Prabakar *et al*., 2012). Often the disease is not present around all twelve clock hours, so a description may often refer to "x" number of clock hours of disease (e.g., nine clock hours would mean that three quarters of the circumference of the retina is involved).

In general, the supervised algorithms that integrate the use of training images and classifiers have been reported for better segmentation results of retinal vessel and ridge at the cost of higher computation times. The manual segmentation of a single training image has more difficult and time consuming process, although this process somewhat mitigated if hand-segmenting only a portion of an image has been sufficient to train the classifier. In many cases of retinal images this

efficient supervised algorithms could not be used to transform or enhance the image, because of huge variations at the image acquisition and health of the subject. So that simple thresholding operation could be used to identify the retinal vessels and ridges then more sophisticated classifiers have to be used for the decision making process (Julien *et al*., 2003).

On the other hand, unsupervised algorithms have been often utilized for this application to obtain faster result and can be tested easily on new image types without any need for training sets to be generated. But the primary disadvantage of this algorithm is that they often use filters and operations that have been tailored for a particular type or resolution of image and can require significant modifications to be applied to others. In some cases of manually segmented training images, this algorithm introduced the requirement of the fundamental approach of preprocessing followed by thresholding typically used with unsupervised algorithms has been combined with the automatic optimization of parameters (Robert *et al*., 2012; Lassada *et al*., 2004).

The present unsupervised algorithm development work for ROP screening has two stages using Wavelet schemes such as the first stage deals with the detection of the blood vessels, measuring the tortuosity and vessel width from the retinal fundus image by the third level decomposition and then the proceeding stage as forth level decomposition deals with the ridge location and width estimation in various zone of the retina. Thus the parameters such as tortuosity, vessel and ridge width have been utilized to detect the disease such as ROP severity levels have been estimated. The proposed method has been utilized to screen the severity level of the disease in automatic machine vision algorithms to reduce the present manual investigation by the ophthalmologists. Hence the manual detection of the tortuosity, vessel and ridge width and severity level of the disease is time consuming and the ophthalmologist may intend to repetitive stress injury on scanning and analyzing the fundus images (Robert *et al*., 2012). This study will act as tool to analyze the diseased by non ophthalmologists.

LITERATURE SURVEY ON RETINOPATHY DETECTION

Automated fundus image analysis plays an important role in the computer aided diagnosis of ophthalmologic disorders. A lot of eye disorders, as well as cardio-vascular disorders, are known to be related with retinal vasculature changes. Many studies have been done to explore these relationships. However, most of the studies are based on limited data obtained using manual or semi-automated methods due to the lack of automated techniques in the measurement and analysis of retinal vasculature. The relationship between changes in retinal vessel morphology and the onset and progression of diseases such as diabetes, hypertension and Retinopathy of Prematurity (ROP) has been the subject of several large scale clinical studies. However, the difficulty of quantifying changes in retinal vessels in a sufficiently fast, accurate and repeatable manner has restricted the application of the insights gleaned from these studies to clinical practice. Detecting blood vessels in retinal images with the presence of bright and dark lesions is a challenging unsolved problem.

Benson *et al*. (2010), has proposed a novel multi-concavity modeling approach to handle both healthy and unhealthy retinas simultaneously. The differentiable concavity measure and the line-shape concavity measure have been proposed to handle bright lesions in a perceptive space and to remove dark lesions which have an intensity structure different from the line-shaped vessels in a retina, respectively. The locally normalized concavity measure has been designed to deal with unevenly distributed noise due to the spherical intensity variation in a retinal image. These concavity measures are combined together according to their statistical distributions to detect vessels in general retinal images. They have obtained very encouraging experimental results that the proposed method consistently yields the best performance over existing state-of-the-art methods on the abnormal retinas and its accuracy outperforms the human observer, which has not been achieved by any of the state-of-the-art benchmark methods. Most importantly, unlike existing methods, the proposed method shows very attractive performances not only on healthy retinas but also on a mixture of healthy and pathological retinas.

Michal and Stewart (2005) have proposed a new technique for extracting vessels in retinal images by the motivation of improving detection of low-contrast and narrow vessels and eliminating false detections at non-vascular structures. The core of the technique has a new likelihood ratio test that combines matched filter responses, confidence measures and vessel boundary measures. Matched filter responses have been derived in scale-space to extract vessels of widely varying widths. A vessel confidence measure is defined as a projection of a vector formed from a normalized pixel neighborhood onto a normalized ideal vessel profile. Vessel boundary measures and associated confidences have been computed at potential vessel boundaries. Combined, these responses form a 6-dimensional measurement vector at each pixel. A learning technique has been applied to map this vector to a likelihood ratio that measures the "vesselness" at each pixel. Results comparing this vesselness measure to matched filters alone and to measures based on the intensity Hessian show substantial improvements both qualitatively and quantitatively. When the Hessian is used in place of the matched filter, similar but less-substantial improvements have been obtained. Finally, the new vesselness likelihood ratio has been embedded into a vessel tracing framework, resulting in an efficient and effective vessel extraction algorithm.

Tortuosity is one of the first manifestations of many retinal diseases such as those due to Retinopathy of Prematurity (ROP), hypertension, stroke, diabetes and cardiovascular diseases. An automatic evaluation and quantification of retinal vessel tortuosity would help in the early detection of such retinopathies and other systemic diseases. Rashmi and Uyyanonvara (2012) have proposed a new approach based on Principal Component Analysis (PCA), for the evaluation of tortuosity in vessels extracted from digital fundus images. One of the strength of the proposed algorithm is that the index is independent of translation, rotation and scaling. Measures are adopted such that the proposed approach matches with the clinical concept of tortuosity. The algorithm is compared with other available tortuosity measures. We have demonstrated its validity as an indicator of changes in morphology using simulated shapes. It is superior to other putative indices, presented previously in literature.

Fraz *et al*. (2012) have presented an automatic evaluation and quantification of tortuosity for the diagnosis of several ocular and systemic diseases which is significant for the clinical recognition of abnormal retinal tortuosity. Two tortuosity evaluation approaches such as Numerical Integration Method (NIM) and Numerical Differentiation Method (NDM) based on continuous curvature to a dataset of 45 infant fundus images have been proposed. Performance evaluation has been done on classification accuracy of three classifiers such as Naive Bayesian classifier, k-nearest neighbor classifier and K-means clustering algorithm, by comparing the estimated results against ground truth from expert ophthalmologists. Results show that different numerical methods provide different tortuosity values for same retinal vessels however have the potential to detect and evaluate abnormal retinal curves. The best classification accuracy of 87.3% has been achieved by the method K-nearest neighbor classifier.

The quantitative analysis of expert opinions have been utilized to demonstrate a methodology for generating composite wide-angles of plus disease in Retinopathy of Prematurity (ROP) proposed (Michael *et al*., 2008). Thirty-four wide-angle retinal images were independently interpreted by 22 ROP experts as "plus" or "not plus." All images were processed by the computer-based Retinal Image multi-Scale Analysis (RISA) system to calculate two parameters: Arterial Integrated Curvature (AIC) and Venous Diameter (VD). Using a reference standard defined by expert consensus, sensitivity and specificity curves were calculated by varying the diagnostic cutoffs for AIC and VD. From these curves, individual vessels from multiple images were identified with particular diagnostic cutoffs and were combined into composite wide-angle images using graphics-editing software. The values associated with 75% under diagnosis of true plus disease (i.e., 25% sensitivity cutoff) were AIC 0.061 and VD 4.272, the values associated with 50% under diagnosis of true plus disease (i.e., a 50% sensitivity cutoff) were AIC 0.049 and VD 4.088 and the values associated with 25% under diagnosis of true plus disease (i.e., 75% sensitivity cutoff) were AIC 0.042 and VD 3.795. Composite wide-angle images were generated by identifying and combining individual vessels with these characteristics. Computer-based image analysis permitted quantification of retinal vascular features and a spectrum of abnormalities is seen in ROP. Selection of appropriate vessels from multiple images can produce composite plus disease images corresponding to expert opinions. This method may be useful for educational purposes and for development of future disease definitions based on objective, quantitative principles.

Peter *et al*. (2012) has been presented a novel algorithm for the fast efficient detection and measurement of retinal vessels, which is general enough that it can be applied to both low and high resolution fundus photographs and fluorescein angiograms upon the adjustment of only a few intuitive parameters. Initially they described the simple vessel segmentation strategy, formulated in the language of wavelets that has been used for fast vessel detection. The proposed method validation using a publicly available database of retinal images, this segmentation achieves a true positive rate of 70.27%, false positive rate of 2.83% and accuracy score of 0.9371. Vessel edges have then more precisely localized using image profiles computed perpendicularly across a spline fit of each detected vessel centreline, so that both local and global changes in vessel diameter can be readily quantified. They observed that the output of their algorithm using second image database have displayed good agreement with the manual measurements made by three independent observers and it produced improved speed and generality without sacrificing accuracy.

Carmen and Domenico (2011) have proposed Unsupervised Segmentation of Retinal Vessels using clustering algorithms such as Self-Organizing Maps (SOM), K-means clustering and Fuzzy C-means clustering. These methods have the advantage that they use knowledge about the vessel network morphology like the most accurate supervised methods, but are completely unsupervised as they do not have any a priori knowledge about the labels of the pixels that they want to classify as vessel or non-vessel. Another advantage of the proposed methods is their fast computational time, compared to supervised methods which are computationally more expensive. The algorithm's segmentation performance has slightly higher accuracy than some benchmark unsupervised algorithms, with slightly lower kappa value than some algorithms on the DRIVE database. The mean accuracy of 0.9347 with a standard deviation of 0.0152 and a mean kappa value of 0.6170 are the outcomes of this algorithm and the ROC curves have shown effective detection of retinal blood vessels (i.e., sensitivity of 69.63) with a small false detection rate (i.e., 1-specificity of 4.21).

Many retinal diseases are characterized by changes to retinal vessels. For example, a common condition associated with Retinopathy of Prematurity (ROP) is so-called plus disease, characterized by increased vascular dilation and tortuosity. Conor *et al*. (2002) have developed a general technique for segmenting out vascular structures in retinal images and characterizing the segmented blood vessels. The segmentation technique had several steps. Initially, morphological preprocessing and second derivative operator have been used to emphasize linear structures such as vessels and thin vascular structures respectively and has been followed by a final morphological filtering stage. Then the thresholding has been used to provide segmented vascular mask. The skeletonisation of this mask has been allowed to identify the points in the image where vessels cross (bifurcations and crossing points) and allowed the width and tortuosity of vessel segments to be calculated. The accuracy of the segmentation stage is quite dependent on the parameters used, particularly at the thresholding stage. However, reliable measurements of vessel width and tortuosity were shown using test images. Using these tools, a set of images drawn from 23 subjects being screened for the presence of threshold ROP disease has been considered. Of these subjects, 11 subsequently required treatment for ROP, 9 had no evidence of ROP and 3 had spontaneously regressed ROP. Applying a simple retrospective screening paradigm based solely on vessel width and tortuosity yields a screening test with a sensitivity and specificity of 82 and 75%.

Vessel enhancement is an important preprocessing step in accurate vessel-tree reconstruction which is necessary in many medical imaging applications. Conventional vessel enhancement approaches used in the literature are Hessian-based filters, which are found to be sensitive to noise and sometimes give discontinued vessels due to junction suppression. A novel framework for vessel enhancement for angiography images has been proposed by Phan *et al*. (2009). The proposed approach incorporates the use of line-like directional features present in an image, extracted by a directional filter bank, to obtain more precise Hessian analysis in noisy environment and thus can correctly reveal small and thin vessels. Also, the directional image decomposition has been helped to avoid junction suppression, which in turn, yields continuous vessel tree. Qualitative and quantitative evaluations performed on both synthetic and real angiography images show that the proposed filter generates better performance in comparison against two Hessian-based approaches.

Julien *et al*. (2003) developed a new tool to assess retinopathy of prematurity. This method has been used geometric information by considering blood vessels as tubes and better supports more complex measures on the extracted data such as tortuosity and dilation. Based on the extracted vessels, the four quadrants of the retina are identified and then a grade is determined via classification using a trained neural network. These techniques extract and quantify both tortuosity and dilation of blood vessels with a sensitivity of 80 and 92% of specificity compared with the prediction of experts.

Fundus image analysis is playing an important role in the early detection of retinal eye diseases like diabetic retinopathy, glaucoma etc. Automated detection of Hypertensive Retinopathy (HR) is also a recent development in this field. Segmentation of blood vessels, measurement of tortuosity, diameter measurement, finding the Artery Vein Ratios (AVR) are few important measures for finding HR using digital fundus images. Kevin and Nayak (2012) have been proposed a support system to assist the ophthalmologist in detecting HR in early stages using fundus images. Segmentation of blood vessels has been done using Radon transform, optic disk has also detected by Hough transform and then the AVR has been estimated. The proposed support system will help the ophthalmologist in the early detection of HR.

Xiayu (2012) has presented a fully automated retinal vessel width measurement technique for delineation and quantitative analysis of blood vessels in retinal fundus image. The accurate vessel boundary delineation problem has been modeled in two-dimension into an optimal surface segmentation problem in three-dimension. Then the optimal surface segmentation problem has been transformed into finding a minimum-cost closed set problem in a vertex-weighted geometric graph. The problem has modeled differently for straight vessel and for branch point because of the different conditions in straight vessel and in branch point. Furthermore, many of the retinal image analysis needed the location of the optic disc and fovea as prerequisite information. Hence, a simultaneous optic disc and fovea detection method has been presented, which included a two-step classification of three classes which have been represented as:

- Developing a fully automated vessel width measurement technique for retinal blood vessels
- Developing a simultaneous optic disc and fovea detection method
- Validating the methods using multiple datasets
- Applying the proposed methods in multiple retinal vasculature analysis studies

Retinal image analysis is an essential step in the diagnosis of various eye diseases. Diabetic Retinopathy (DR) is globally the primary cause of visual impairment and blindness in diabetic patients. Diabetic Retinopathy (DR) is an eye disease caused by the complication of diabetes. Two types of DR are Non-Proliferative Diabetic Retinopathy (NPDR) and Proliferative Diabetic Retinopathy (PDR). Early diagnosis through regular screening and timely treatment has proven beneficial in preventing visual impairment and blindness. Shaeb and Satya (2008) have proposed a

novel approach to automatically detect diabetic retinopathy from digital fundus images. The digital fundus images have been segmented employing morphological operations to identify the regions showing signs of diabetic retinopathy such as hard exudates, soft exudates and the red lesions: micro aneurysm and haemorrhages. Various color space values of the segmented regions have been calculated. A fuzzy set has formed with the color space values and fuzzy rules have been derived based on fuzzy logic reasoning for the detection of diabetic retinopathy.

Diabetic Retinopathy (DR) diagnosis using Machine Learning Techniques would also be the prominent method in recent days. Three models like Probabilistic Neural Network (PNN), Bayesian Classification and Support Vector Machine (SVM) were used and their performances have been compared to detect DR. The features like blood vessel, haemmorages of NPDR images and exudates of PDR images were extracted from the raw images using the image processing techniques and fed to the classifiers for classification. SVM classifier delivered a better result compared with other techniques.

Retinal blood vessels are important structures in ophthalmological images. Many detection methods are available, but the results are not always satisfactory. Vermeer *et al*. (2004) has presented a novel model based method for blood vessel detection in retinal images. It is based on a Laplace and thresholding segmentation step, followed by a classification step to improve performance. The last step assured incorporation of the inner part of large vessels with specular reflection. The method gives a sensitivity of 92% with a specificity of 91%.

Retinopathy of Prematurity (ROP) is a common retinal neovascular disorder of premature infants. It can be characterized by inappropriate and disorganized vessel. To determine, with novel software, the feasibility of measuring the tortuosity and width of retinal veins and arteries from digital retinal images of infants at risk of Retinopathy of Prematurity (ROP) an innovative technique has been proposed by Wilson *et al*. (2008). The Computer-Aided Image Analysis of the Retina (CAIAR) program was developed to enable semiautomatic detection of retinal vasculature and measurement of vessel tortuosity and width from digital images. To measure tortuosity a multi-scale approach that successively subdivided vessel sections into two parts has been adopted. The geometric concept involved perpendicular bisection of the vessel chord at its midpoint and subsequent reapplication of the subdivision on the resultant segments until the segment lengths fall below a specified value (4 pixels). Two methods were used to estimate width: First method estimated from the maximum-likelihood model fitting. This is the standard deviation of the Gaussian profile that was fitted at that location. Second, the correlated measure of isotropic contrast at the vessel centerline has been computed by the response of a Laplacian of Gaussian (LoG) filter. CAIAR was tested for accuracy and reproducibility of tortuosity and width measurements by using computer-generated vessel-like lines of known frequency, amplitude and width. CAIAR was then tested by using clinical digital retinal images for correlation of vessel tortuosity and width readings compared with expert ophthalmologist grading. CAIAR offers the opportunity to develop an automated image analysis system for detecting the vascular changes at the posterior pole, which are becoming increasingly important in diagnosing treatable ROP.

Lassada *et al*. (2004) have presented a method for blood vessel detection on infant retinal images. The algorithm has been designed to detect the retinal vessels. The proposed method applied a Laplacian of Gaussian as a step-edge detector based on the second-order directional derivative to identify locations of the edge of vessels with zero crossings. The procedure allowed parameters computation in a fixed number of operations independent of kernel size. This method has been composed of four steps: grayscale conversion, edge detection based on LOG, noise removal by adaptive Wiener filter and median filter and Otsu's global thresholding. The algorithm has done well to detect small thin vessels, which are of interest in clinical practice.

MATERIALS AND METHODS

The related work review described many clinical procedures and imaging algorithms to investigate the Retinopathy of Prematurity disease stages. All the proposed methods have its own merits and de merits according to the application on ROP image analysis. To overcome the disadvantages and efficient quantification of retinal vessels and ridges presented in the ROP images, a new wavelet based methodology has been proposed in this study. The implementation of this algorithm has been delivered the various parameters of retinal vessels and ridges to efficiently screen the severity stage of ROP.

The premature infant retinal images obtained from pediatric section of an eye hospital in the south Indian region. The digital retinal images have been captured by RetCam-120; MLI Inc., Pleasanton, California at 45° field of view. Generally minimum 5 retinal images for each right and left eye of the premature infants have been collected and considered for the present algorithm accomplishment. These raw color images are in .hdr or .bmp format with a size of 640×480 pixels. In all cases, color images have been converted to grayscale by extracting the green channel information and treating this as containing gray levels, because the green channel has revealed the best contrast for vessel detection.

Before the gray scale conversion of the color retinal image, the brightness, color and contrast of the image have been enhanced with the mean intensity adjustment and contrast stretching method. This process has improved the appearance of retinal blood vessel and

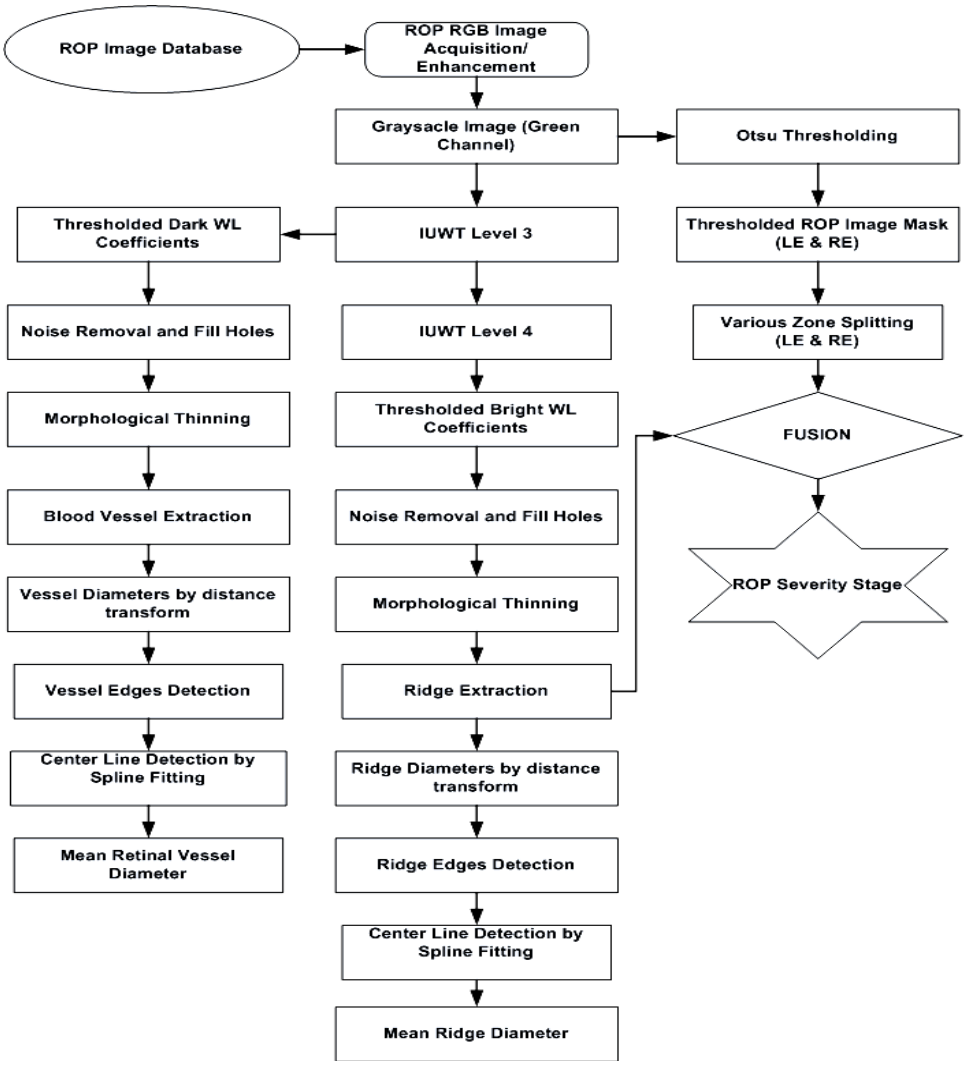

Fig. 3: General block diagram of wavelet based ROP screening system

ridge formation. Further a minimized mask has been created to exclude the unnecessary parts of the image in processing which has been improved the accuracy level on the boundary detection.

Then the two dimensional Isotropic Un-decimated Wavelet Transform (IUWT) has been proposed for the gray scale ROP images to analyze the blood vessel by third iteration and ridges by fourth iteration as shown in Fig. 3. Consecutively the dark vessel thresholding (16-20%) or bright vessel thresholding (13-17%) have been applied to the iterated ROP images to extract the retinal vessel and ridges respectively. The various numerical parameters of the segmented vessel and ridge have been measured by different mathematical computations. The thresholding technique has been utilized to develop the retinal mask and defined the various zones of the retina. The optic disk and fovea localization has been obtained to define the exact zones in the retina. Then the fusion of extracted ridge with zones and diameter of the ridge information has delivered the proper severity stage of the ROP.

Two dimensional isotropic un-decimated wavelet transform: Recent past multi-scale methods plays a vital role and have become very popular, especially with the expansion of wavelets. Generally Decimated bi-orthogonal Wavelet Transform (DWT) has been used in many medical image applications. But DWT has loss of translation invariance property, which leads to a large number of artifacts in its resultant image i.e., when an image has been reconstructed after modification by its wavelet coefficients. So that DWT technique is not mostly preferred for analysis of data. Starck *et al*. (1998) and Starck and Murtagh (2001, 2002, 2007) have been proposed the thresholding using an un-decimated transform rather than a decimated one can improve the result by more than 2.5 dB in denoising applications.

The undecimated wavelets transform and its reconstruction consists of the standard un-decimated wavelet transform and the Isotropic Un-decimated Wavelet Transform (IUWT). In which, the Isotropic Un-decimated Wavelet Transform (IUWT) is a

powerful, redundant wavelet transform that has been used in astronomy and biology applications (Antoine and Murenzi, 1994; Dutilleux, 1989). The un-decimated wavelet transform, particularly IUWT and its reconstruction has been described in this section. Then the specially designed filter banks has been presented for IUWT decompositions which have some useful properties such as being robust to ringing artifacts which appear generally in wavelet-based denoising methods extremely useful for ROP images.

The IUWT algorithm has been well known for the astronomical domain and biological functions especially retinal image analysis, because it is well adapted to the images where objects are more or less isotropic in most cases. Requirements for a good analysis of such data are as follows.

Filters must be symmetric:

$$\bar{h}[k] = h[k] \text{ and } \bar{g}[k] = g[k] \quad (1)$$

In 2-D or higher dimension, h, g, ψ, ϕ must be nearly isotropic.

For a real discrete-time filter whose impulse response is h[n], $\bar{h}[n] = h[n], n \in \mathbb{Z}$ is its time reversed version. For wavelet representation, analysis filters are denoted as h and g. The scaling and wavelet functions using for analysis are denoted as ϕ and ψ, respectively. Filters need not be orthogonal or bi-orthogonal and this property such as the lack of the need of orthogonality or bi-orthogonolity is the advantageous for design freedom. So, the separability; h[k, l] = h[k]h[l] has been considered for the fast calculations for huge volume of data set. This implementation has appreciated by wavelet theory at each iteration i, scaling coefficients c has been computed by low pass filtering and and wavelet coefficients w_i by subtraction.

The analysis of scaling and wavelet functions has preferred the following:

$$\phi_1(x) = \frac{1}{12}(|x-2|^3 - 4|x-1|^3 + 6|x|^3 - 4|x+1|^3 + |x+2|^3) \quad (2)$$

$$\phi_1(x, y) = \phi_1(x)\,\phi_1(y) \quad (3)$$

$$\frac{1}{4}\psi\left(\frac{x}{2}, \frac{y}{2}\right) = \phi(x, y) - \frac{1}{4}\phi\left(\frac{x}{2}, \frac{y}{2}\right) \quad (4)$$

where, $\phi_1(x)$ is the spline of order 3 and the wavelet function is defined as the difference between two resolutions. The related filters h and g is defined by:

$$h^{1D}[k] = \frac{[1,4,6,4,1]}{16}, k = -2, \ldots, 2 \quad (5)$$

$$h[k, l] = h^{(1D)}[k]h^{(1D)}[l] \quad (6)$$

$$g[k, l] = \delta[k, l] - h[k, l] \quad (7)$$

where, δ is defined as $\delta[0, 0] = 1$ and $\delta[k, l] = 0$ for all (k, l) different from $(0, 0)$.

The mean of the original signal has been preserved by the scaling coefficients. But the wavelet coefficients have a zero mean and information have been encoded for the corresponding different spatial scales present within the signal. This has been applied to a signal c_0 and the subsequent scaling coefficients are calculated by convolution with a filter h^{ui}:

$$c_i = c_i * h^{ui} \quad (8)$$

where, the filter $h_0 = [1, 4, 6, 4, 1]/16$ is derived from the cubic B-spline and h^{ui} is the up sampled filter obtained by inserting $2^i - 1$ zeros between each pair of adjacent coefficients of h_0. The filtering has to be applied in all directions when the original signal c_0 is multidimensional.

The Finite impulse response filters $(h, g = \delta - h)$ should follow certain properties to characterize any pair of even symmetric analysis. For any pair of even symmetric filters h and g such that $g = \delta - h$, has to comply with the following symmetric properties:

- This FIR filter bank implements frame decomposition and perfect reconstruction using FIR filters should be possible.
- A tight decomposition should not implement with the above filters.

Based on the structure of g, the wavelet coefficients have been obtained by calculating the difference between two resolutions, which is:

$$\omega_{i+1}[k, l] = c_i[k, l] - c_{i+1}[k, l] \quad (9)$$

where,

$$c_{i+1}[k, l] = (\bar{h}^{(j)}\bar{h}^{(j)} * c_i)[k, l]$$

This simple difference between two adjacent sets of scaling coefficients represented as wavelet coefficients i.e.:

$$w_{i+1} = c_i - c_{i+1} \quad (10)$$

One set of $\{w_i\}$ could be obtained for each scale of i, which has the same number of pixels as the input image. The reconstruction has been obtained by simple co-addition of all wavelet scales and the final smoothed array:

$$c_0[k, l] = c_j[k, l] + \sum_{i=1}^{I} w_i[k, l] \quad (11)$$

So the reconstruction of the original signal from all wavelet coefficients and the final set of scaling

coefficients required addition only. After the computation of n wavelet levels:

$$c_0 = c_n + \sum_{i=1}^{n} w_i \quad (12)$$

The synthesis filters $\tilde{h} = \delta$ and $\tilde{g} = \delta$ are FIR based on the symmetric filter properties. This wavelet transformation has been adopted for the analysis of ROP images which contain the isotropic objects.

The set of wavelet coefficients generated at each iteration have been referred to as a wavelet level and the larger features such as the retinal vessels and ridges have become visible with improved contrast on higher wavelet levels. Especially wavelet level 3 has been adopted for better blood vessel visibility and level 4 to visualize the ridges on the ROP images. The wavelet levels which exhibit the best contrast have been added and the thresholding have also been applied to lowest valued coefficients to carry out the segmentation of vessels in ROP images. The Field of View (FOV) has been estimated for a ROP image and the thresholds have been computed from pixels within the FOV. In order to ensure that the dark pixels outside FOV did not considered for the threshold computation. When the non availability of FOV mask, the global threshold has been applied to the ROP images and this become the best method applied to green channel images.

The wavelet levels and thresholds need not be changed for all the fixed size of retinal images. But to extract the blood vessel from all ROP images (both low and high resolution) the wavelet level has to be chosen to third level decomposition and the threshold has to be fixed as 18-23% of lowest coefficients. Similarly to extract the ridges from the ROP images the wavelet levels and threshold have been chosen to fourth level and 15%, respectively and also the inverted binary image has been preferred to obtain the perfect ridge.

Vessel width and ridge width measurement: The vessel width and ridge width measurement strategy consist two stages of processing first is the vessel or ridge middle line estimation and the second is the edge identification of vessel and ridge. The morphological thinning algorithm has been proposed to extract the middle line of the vessel and ridge. Thinning has iteratively removed exterior pixels from the detected vessels, finally resulting in a new binary image containing connected lines of ‘on’ pixels running along the vessel centers. The end pixels which have <2 neighbors have been identified and the branch The ROP severity has various stages from stage 1 to stage 5, plus disease and Aggressive Progressive ROP. In which we have considered the ROP images up to stage 3 and plus diseased for the current screening process. Obviously the stage 4 and stage 5 are the most severe stage and the baby may not get the vision properly even though the proper clinical procedures are following to treat the same with utmost care. The IUWT has been applied for stage 1 to stage 3 ROP images and extracted the ridges by the fourth level of Wavelet decomposition and threshold has been defined to 15% with bright vessel selection. Since almost all the cases the ridges have been looking brighter than other locations. If the ridges have been compared with retinal vessels in the ROP images, they have inverse intensity and resolution property of the images.

The pixels which have >2 neighbors been removed. Many monotonous middle lines have been eliminated as much as possible by removing the short segments which have <10 pixels. So that unwanted spur which produced side-effect on thinning process and end bifurcated vessels i.e., vascular tree into individual vessel segments have also been eliminated. A coarse estimate of vessel widths have been calculated using the distance transform of the inverted binary segmented image especially on ridge segmentation. Finally the connected group of pixels represented the middle line of a potential vessel segment which could be used for further analysis.

The orientation of a vessel segment at any point could be estimated directly from its middle line, but discrete pixel coordinates have not been well suited for the computation of angles. A least-squares cubic spline or in piecewise polynomial form for any orientation of a vessel has been fitted to each middle line to combine some smoothing with the ability to evaluate accurate derivatives at any location. The smooth middle line could be obtained by using a parametric spline curve based on the centripetal scheme described by Lam *et al*. (1992) and Lee (1989).

The measurement of vessel and ridge widths required the location of edge points, but these have no unique description within the image space. The ROP vessel and ridge profiles have resemblance of Gaussian functions; generally edges have previously been defined in different methods, including using gradients or model fitting. The presence of central light reflex is one of the major impediments while development of vessel width measurement strategy. It has been visualized as a ‘dip’ or ‘hill’ approximately in the center of the vessel and ridge profile and which has been more likely to be found in higher resolution images and wider vessels. Some of the vessel and ridge measurement algorithms have misidentified the light reflex as the vessel or ridge edge have been reported as challenging task and explicit strategies for dealing with this issue have to ensure that any measurement should be adequately robust (Lee, 1989). The edge has been occurred at a local gradient maximum or minimum as identified to sub-pixel accuracy using the zero-crossings of the second derivative otherwise which has been defined as the rising edge and the falling edge.

The average vessel or ridge width has been estimated from the binary profiles. The sum of ‘vessel’

pixels in each profile has been computed and the median of these sums have been taken as the provisional width. Then the average of all the vessel profiles have been calculated and identify the locations of the maximum and minimum gradient to the left and right of the centre respectively, bounded to a search region of one estimated width from the centre. These locations have given the columns in the vessel profile images at which edges have been predicted to fall. The distance between the two columns also gave a more refined and robust estimate of mean vessel width, largely independent of the thresholds used for the initial segmentation (Olivo-Marin, 2002). An anisotropic Gaussian filter have been applied to the vessel profiles image to reduce noise and then a discrete estimate of the second derivative perpendicular to the vessel by finite differences have been calculated. Then locations where the sign of the pixels in each filtered profile changes have been identified and categorized these based upon the direction of the sign change into potential left and right vessel edges. Using connected components labeling, the possible edges into distinct trails have been linked. Then the trails that never come within 1/3 of an estimated vessel diameter from the corresponding predicted edge columns have been removed. Finally the zero-crossings belonging to the longest remaining trails to each side of the vessel centre have been estimated as edges and the diameter has simply the Euclidean distance between these edges (William *et al*., 1999).

RESULTS AND DISCUSSION

This proposed work involved two main steps, the much faster unsupervised vessel and ridge segmentation by thresholding wavelet coefficients have been implemented as the first step, which would achieve better accuracy and less computation time compared with the other existing techniques. The second step has included a new alternative to the graph-based algorithm to extract middle lines and locate the vessel and ridge edges from ROP image profiles. This could be achieved by using the spline fitting to determine vessel orientations and then detecting the zero crossings of the second derivative perpendicular to the vessel and ridge.

The IUWT has been performed somewhat extraordinary as a wavelet transform and has a particularly straightforward implementation. The efficient means of combining background subtraction along with noise and high-frequency content inhibition using an approximately Gaussian filter have become the outcomes of IUWT execution on ROP images. So that, the wavelet coefficients resemble the values that would be computed directly using a difference of Gaussian's filter. It would be well suited for the tasks of accurate retinal vessel and ridge segmentation, detection and measurement by this algorithm, despite of its cleanness.

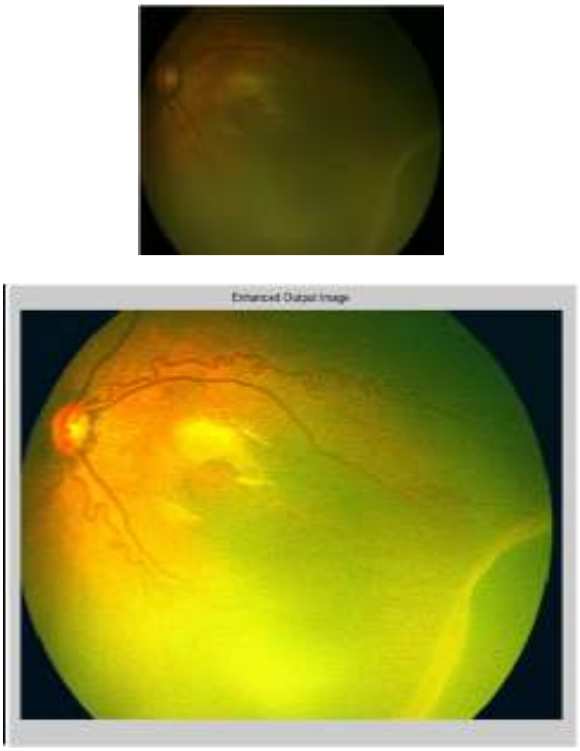

Fig. 4: Original RetCam ROP image and contrast enhanced image

The present work considered 28 premature infants who have the ROP issues at various stages. Each infant's retinal images have been acquired with RetCam at the Pediatric Ophthalmology center, in the Coimbatore location using regular ROP screening procedures. For every infant the ophthalmologists have been considered minimum five images or some cases which may be increased up to 8 images/eye to analyze the exact stage of ROP. The ophthalmologist's proficiency level plays a vital role in ROP severity screening. Based on the clinical features of ROP images, the IUWT have been adopted for left eye and right eye images to extract the vessels and ridges and measure the widths. The ROP images obtained from RetCam are in .hdr or .bmp file format with the size of 640×480. These unprocessed images have been preprocessed and enhance contrast of the retinal vessels and ridges as shown in Fig. 4. These images have been considered as the input for the proposed IUWT based system.

The various IUWT iteration levels have been applied for the input ROP images and observed that the level 3 iteration has delivered the satisfied output. Then the dark thresholding have been selected to 20% to extract the dark blood vessels. The output has more unwanted noise, so that the simple morphological functions such as erosion, dilation, connectivity and blob filling techniques have been utilized to obtain the optimum retinal vessel structures as shown in Fig. 5.

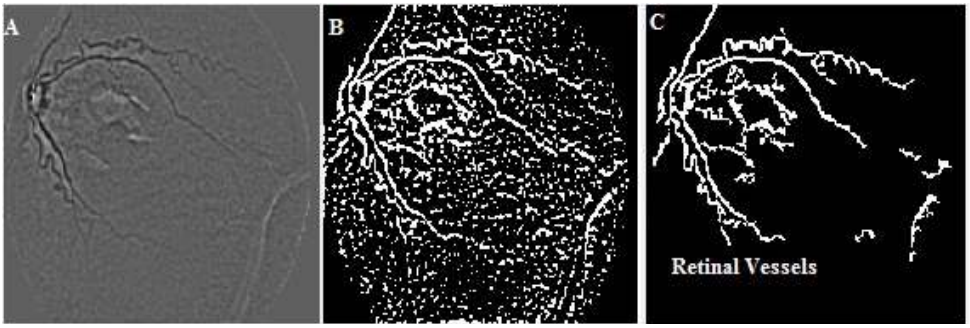

Fig. 5: A) IUWT level 3 applied image, B) thresholded image, C) segmented retinal vessels

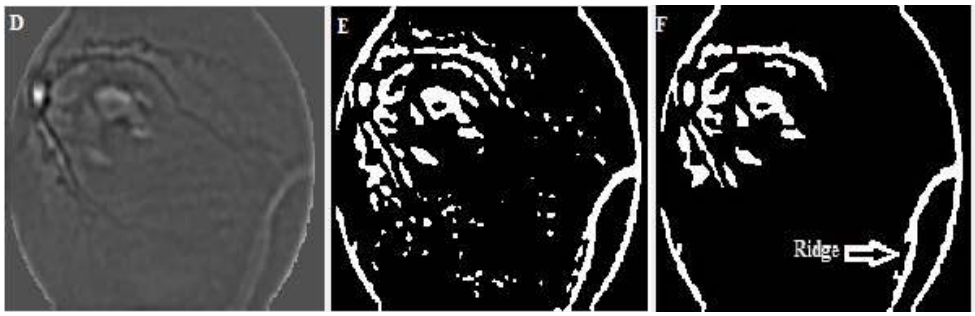

Fig. 6: D) IUWT level 4 applied image, E) bright thresholded image, F) segmented ridge structure

Table 1: Various properties of stage 1 ridge measurement

Stage 1 ridge measurement								
Case	Eye	No of widths	Mean width (mm)	S.D.	Min. ridge width (mm)	Max. ridge width (mm)	Ridge length (mm)	Tortuosity
1	LE	150	1.2565	0.3453	0.5698	1.8546	40.2521	1.0426
	RE	224	1.8739	0.6387	0.5863	3.1948	61.1355	1.4863
2	LE	36	0.9281	0.2379	0.5562	1.3894	9.8343	1.0426
	RE	56	2.4762	0.2722	1.9707	3.0259	14.6168	1.0373
3	LE	75	1.4324	0.3834	0.6698	2.2404	22.0379	1.7674
	RE	39	0.9860	0.3906	0.4614	1.5760	11.3950	1.0014
4	LE	27	2.5868	0.4526	2.1369	3.5550	7.6361	1.0139
	RE	154	3.0761	0.8193	1.6144	4.9752	41.3855	1.1154
5	LE	32	1.4758	0.2811	0.8311	2.0621	14.0854	1.0372
	RE	32	2.7008	0.3904	2.2960	3.4052	8.1493	1.0268
6	LE	66	1.6279	0.5722	1.0049	2.7470	17.2139	1.0353
	RE	40	2.8902	0.4635	2.5172	4.0160	10.4776	1.0627
7	LE	42	1.3230	0.4044	0.5615	1.8969	12.1323	1.0462
	RE	47	2.2613	0.5299	0.9300	3.1178	11.8788	1.2101
8	LE	31	2.0188	0.5628	0.9202	2.6923	10.0124	1.0167
	RE	27	1.4944	0.1349	1.2199	1.6646	7.5061	1.0136
9	LE	171	1.7477	0.5694	0.3946	3.1787	52.9401	1.2459
	RE	300	2.1121	0.6290	0.7003	3.3932	86.8941	1.0238

S.D.: Standard deviation; Min.: Minimum; Max.: Maximum

The tortuosity level of the retinal vessels have been estimated for the required vessel portions by manual selection using relative length variation method.

The IUWT iteration has been extended from third level to fourth level to extract the ridges available in the ROP images. In this process, instead of dark thresholding, the bright thresholding has been chosen to 15% to extract the ridges. Then the similar morphological operators have been used to extract the ridges and the ridge portions alone have been selected manual intervention as shown in Fig. 6. In this study, 1 pixel is approximately equivalent to 0.27 mm has been considered to extract the ridge length from the segmented images. Then the properties of a ridge such as maximum and minimum width, mean width, standard deviation and tortuosity levels have been computed to screen the stage of ROP. For each and every stage's various ridge values have been tabulated as shown in Table 1 to 3.

The various parameters such as number of widths, mean width, standard deviation, minimum width, maximum width, ridge length and tortuosity of stage1,

Table 2: Various properties of stage 2 ridge measurement

Stage 2 ridge measurement								
Case	Eye	No of widths	Mean width (mm)	S.D.	Min. ridge width (mm)	Max. ridge width (mm)	Ridge length (mm)	Tortuosity
1	LE	356	1.5567	0.4405	0.5816	2.4556	98.6751	1.3586
	RE	466	1.9771	0.6512	0.4739	3.6394	129.1242	1.1927
2	LE	246	1.9274	0.6171	0.6338	3.5667	66.7943	1.0738
	RE	336	2.7246	0.8241	0.7097	4.4254	90.2561	1.0361
3	LE	137	1.2707	0.3312	0.6372	1.9306	37.8547	1.0238
	RE	317	2.1354	0.7496	0.9501	4.2921	86.2478	1.0604
4	LE	156	5.5231	1.0212	2.9668	7.1383	42.1550	1.0996
	RE	165	5.4279	1.4210	3.4821	8.0491	44.8270	1.1470
5	LE	33	3.0385	0.2071	2.8099	3.4272	9.2086	1.1079
	RE	57	2.8210	0.5750	1.9593	3.9476	19.8108	1.0308
6	LE	250	1.8003	0.6017	0.4965	3.3842	66.9522	1.0605
	RE	112	2.0325	0.7240	0.7245	3.1498	29.2821	1.0219
7	LE	303	2.6150	0.7733	0.4318	4.0229	80.9361	1.0489
	RE	112	2.6314	1.0497	0.6025	4.7064	29.9288	1.8599
8	LE	145	1.6832	0.4940	0.7429	2.7112	39.2842	1.1471
	RE	357	1.3892	0.5496	0.1754	2.6700	110.6390	1.0947
9	LE	134	3.3090	1.1099	1.4049	5.3819	37.4287	1.0468
	RE	259	3.8011	1.3430	1.4925	6.2773	70.2925	1.1839
10	LE	198	1.8817	0.8385	0.4081	3.9992	54.3638	1.1094
	RE	95	1.8679	0.4085	0.7458	2.6647	26.2608	1.1051

S.D.: Standard deviation; Min.: Minimum; Max.: Maximum

Table 3: Various properties of stage 3 ridge measurement

Stage 3 ridge measurement								
Case	Eye	No of widths (mm)	Mean width (mm)	S.D.	Min. ridge width (mm)	Max. ridge width (mm)	Ridge length (mm)	Tortuosity
1	LE	139	5.5142	2.0437	2.5772	9.9167	156.3164	1.3224
	RE	69	5.3912	0.7315	3.7353	6.5336	18.4460	1.0483
2	LE	219	6.5009	2.0079	3.0970	11.2826	316.0073	1.3359
	RE	338	1.2440	0.3847	0.6125	2.3965	91.4554	1.4785
3	LE	118	7.4700	0.7838	6.0497	9.0362	32.8272	1.0515
	RE	254	6.7396	1.5353	3.0328	8.9062	68.1560	1.0520
4	LE	184	3.2598	0.6371	2.0034	4.6751	48.0983	1.0841
	RE	471	4.5965	1.2589	1.4389	6.3851	133.7524	2.9524
5	LE	192	3.3379	1.3022	1.4426	5.9724	52.0834	1.2329
	RE	192	3.1302	0.7198	1.6426	4.7580	57.6215	1.0371
6	LE	168	2.6522	1.0557	0.6989	4.5476	48.9944	1.0179
	RE	134	2.3415	0.5327	1.2345	3.6966	35.5252	1.0953
7	LE	416	2.5721	1.1854	0.8158	6.3361	111.2873	1.1022
	RE	38	5.7070	0.2137	5.2092	5.9663	9.4643	1.0041
8	LE	390	4.1397	1.2984	1.3384	7.2142	104.5571	1.0440
	RE	178	3.9205	0.9196	1.3425	5.7484	48.0624	1.0473
9	LE	148	4.8142	1.5413	2.7642	7.6954	39.9464	1.2096
	RE	148	4.2671	0.9421	2.7325	6.4683	41.2754	1.0485

S.D.: Standard deviation; Min.: Minimum; Max.: Maximum

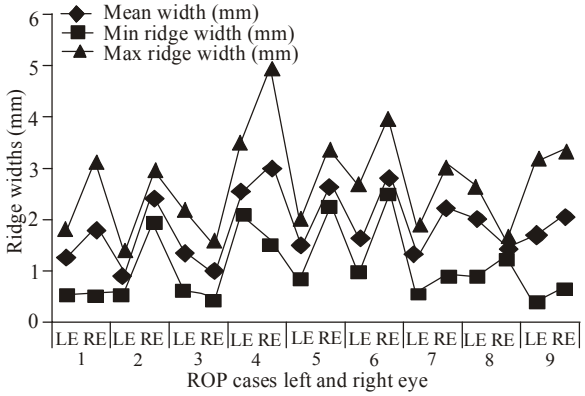

Fig. 7: Stage 1 ridge parameters measurement (mean, minimum and maximum width) for different cases left and right eye

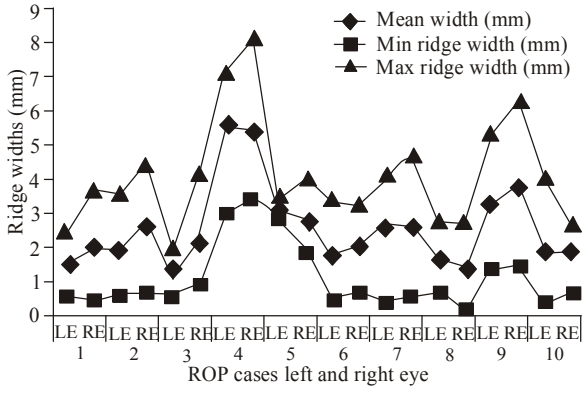

Fig. 8: Stage 2 ridge parameters measurement (mean, minimum and maximum width) for different cases left and right eye

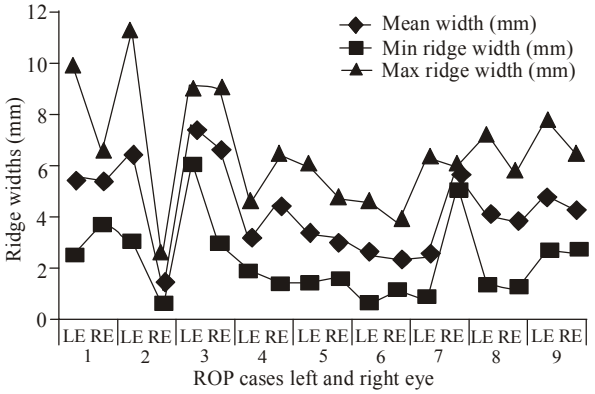

Fig. 9: Stage 3 ridge parameters measurement (mean, minimum and maximum width) for different cases left and right eye

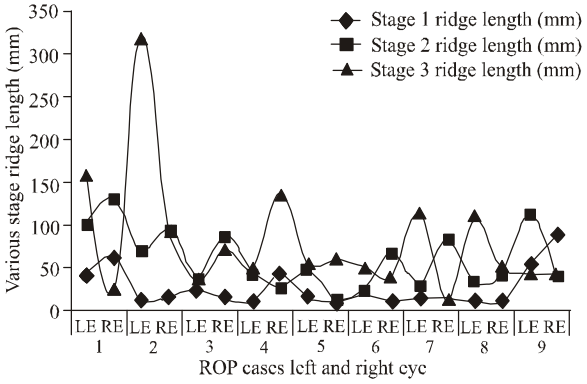

Fig. 10: Various stages ridge length measurement for different cases left and right eye

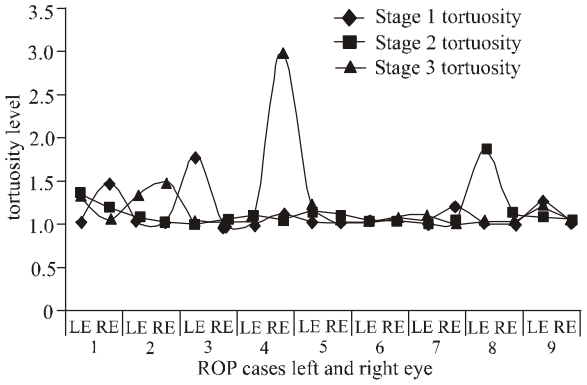

Fig. 11: Various stages ridge tortuosity level measurement for different cases left and right eye

stage 2 and stage 3 for the left and right eye have been measured and tabulated. These values have been contributed very important role in the ROP severity stage screening.

The Fig. 7 to 9 illustrated the ridges mean width, minimum and maximum ridge width versus various cased have the stage 1, stage 2 and stage 3 level of ROP diseases. The stage 3 ridge parameters measurement has highest span of widths starts from 2.3965 to 11.2826 mm. The other two stages such as stage 1 and stage has the maximum ridge width of 4.9752 and 8.0491 mm respectively. The mean ridge width measurements have also been specified that the stage 3 has more predominant value compared with other two stages. Surprisingly, the minimum ridge width measurement indicated that stage 2 has the lowest value i.e., 0.1754 mm when compared with the stage 1 minimum width value i.e., 0.3946 mm.

The ridge length of various stages versus the cases has been shown in the Fig. 10. This represented that the stage 3 has largest ridge length. Similarly the Fig. 11 symbolized that the tortuosity level in various stages of ROP cases which has been depicted the stage 3 has the biggest value. The stage 1 and stage 2 has very low discriminant features when compared with stage 3. So the ROP screening systems considered these ridge parameters and which have been measured for the new input retinal image and categorize the stage accordingly.

CONCLUSION

A fast and accurate unsupervised algorithm to detect and measure blood vessels and ridges in various stages of ROP images have been described in this study. This developed algorithm have been implemented for various stages of ROP images and identified that it could deliver high level of accuracy, low measurement error and short computation time for both low and high resolution images. From the outcomes of the IUWT implementation on ROP images, it is observed that this proposed method is more suitable than the existing techniques.

The various parameters measurement of retinal vessels and ridges for various stages of ROP images has been quantified and further screening has been progressed. Based on the measured parameters, the stage 3 has more significant parameters compared with other stages such as stage 1 and stage 2. From the implementation of this system, we observed that the ROP screening system could be easily identify the stage 3 cases and the system felt fuzziness at stage 1 and stage 2. The ROP severity stage quantification and screening system produced 93% accurate result on stage 3 and 85% accuracy in stage 1 and stage 2. The effectiveness of the proposed method has been demonstrated through experimentation using various ROP diseased cases. The outputs from the developed system have been validated with the results of experts.

The best ROP classification could be achieved by the implementation of efficient soft computing based classifier using the retinal vessel and ridge parameters. The thresholding based retinal image mask can be created to classify the various zones in the retina. The

fusion of the retinal vessels and ridges with retinal mask images could be delivered the proper severity stage of ROP. The work could be extended with these techniques and could achieve better results in future. The Graphical User Interface (GUI) based menu options will also be provided user friendly environment for non ophthalmologist so that the time consumption of ophthalmologists can be considerably reduced i.e., instead of analyzing all RetCam images they provide prominent diagnosis on the infants who have suffered with severe stage ROP.

ACKNOWLEDGMENT

The authors would like to thank Kathir College of Engineering, Coimbatore and Aravind eye hospital, Coimbatore for providing necessary facilities to carry out this study. The suggestions and comments of anonymous reviewers, which have greatly helped to improve the quality of this study, are also acknowledged.

REFERENCES

Antoine, J.P. and R. Murenzi, 1994. Two dimensional wavelet analysis in image processing. Physicalia Mag., 16: 105-134.

Benson L., SY, Yongsheng Gao and Alan Wee-Chung Liew, 2010. "General Retinal Vessel Segmentation Using Regularization-Based Multiconcavity Modeling," IEEE Transactions on Medical Imaging, 29(7): 1369-1381.

Conor, H., J. Flynn, M.O. Keefe and M. Cahill, 2002. Characteriztion of changes in blood vessel width and tortuosity in retinopathy of prematurity using image analysis. Med. Image Anal., 6(4): 407-429.

Carmen A.L. and T. Domenico, 2011. "Automatic Unsupervised Segmentation of Retinal Vessels Using Self-Organizing Maps and K-Means Clustering", Rizzo, R. and P.J.G. Lisboa, Springer Verlag LNBI 6685, pp: 263-274.

Dutilleux, P., 1989. An implementation of the 'algorithme `a trous' to compute the wavelet transform. In: Combes, J.M., A. Grossmann and P.H. Tchamitchian (Eds.), Wavelets: Time-frequency Methods and Phase-space. Springer, New York.

Early Treatment of Retinopathy of Prematurity Cooperative Group, 2003. Revised indications for the treatment of retinopathy of prematurity. Arch Ophthalmol., 121: 1684-96.

Fraz, M.M., P. Remagnino, A. Hoppe, B. Uyyanonvara, A.R. Rudnicka, C.G. Owen and S.A. Barman, 2012. Blood vessel segmentation methodologies in retinal images-A survey. Comput. Methods Programs Biomed., 108: 407-433.

Gwenole, Q., M. Lamard, P.M. Josselin and G. Cazuguel, 2008. Optimal wavelet transform for the detection of micro aneurysms in retina photographs. IEEE T. Med. Imaging, 27(9): 1230-1241.

International Committee for the Classification of Retinopathy of Prematurity, 2005. The international classification of retinopathy of prematurity revisited. Arch Ophthalmol., 123: 991-999.

Julien, J., D.K. Wallace and S. Aylward, 2003. Quantification of retinopathy of prematurity via vessel segmentation. Medical Image Computing and Computer assisted intervention-MICCAI 2003. Springer Lect. Notes Comput. Sci., 2879: 620-626.

Kevin N. and K.P. Nayak, 2012. "A Review of Fundus Image Analysis for the Automated Detection of Diabetic Retinopathy", Journal of Medical Imaging and Health Informatics, 2(3): 258-265(8).

Lam, B.S.Y. and Y. Hong, 2008. A novel vessel segmentation algorithm for pathological retina images based on the divergence of vector fields. IEEE T. Med. Imaging, 27(2): 237-246.

Lam, L., S.W. Lee and C.Y. Suen, 1992. Thinning methodologies-a comprehensive survey. IEEE T. Pattern Anal., 14: 869-885.

Lassada, S., B. Uyyanovara, S.A. Barman and J. Jaruwat, 2004. Automated vessels detection on infant retinal images. Proceeding of International Conference on Control, Automation and Systems, pp: 321-325.

Lee, E.T.Y., 1989. Choosing nodes in parametric curve interpolation. Comput. Aided Design, 21: 363-370.

Michal S. and C.V. Stewart, 2005. "Retinal Vessel Extraction Using Multiscale Matched Filters, Confidence And Edge Measures", Department of Computer Science, Rensselaer Polytechnic Institute, Troy, New York 12180-3590, Technical Report : 05-20.

Michael F.C., E.S. Karen, Y.K. David, W. Lu, A.K. Steven, C. Osode, S. Justin and T.F. John, 2008. "Telemedical Diagnosis of Retinopathy of Prematurity. Intraphysician Agreement between Ophthalmoscopic Examination and Image-Based Interpretation", Ophthalmology; 115(7): 1222-1228.e3.

Mounir, B., M. Johanne and C.C. Gerontis, 2008. Retinopathy of Prematurity. Retrieved from: http://www.emedicine.medscape.com/article/1225022.

Olivo-Marin, J.C., 2002. Extraction of spots in biological images using multistage products. Pattern Recogn., 35: 1989-1996.

Phan T., T.H. Khan, AU, L. Young-Koo, L. Sungyoung and K. Tae-Seong, 2009. 'Vessel enhancement filter using directional filter bank', Computer Vision and Image Understanding, 113(1): 101-112.

Parag, K.S., A. Saurabh, V. Narendran and N. Kalpana, 2011. Retinopathy of prematurity-the new challenge. Retina, 17(4): 23-27.

Prabakar, S., K. Porkumaran, P.K. Shah and V. Narendran, 2012. Optimized Imaging Techniques to Detect and Screen the Stages of Retinopathy of Prematurity. In: Fabiio, S. (Ed.), Human-Centric Machine Vision, pp: 59-80. ISBN: 978-953-51-0563-3, Intech, DOI: 10.5772/26609.

Peter B., S.C. Norman, M.J. Graham and C.M. Tim, 2012. 'Fast Retinal Vessel Detection and Measurement Using Wavelets and Edge Location Refinement', PLoS ONE, e32435, doi: 10.1371/ journal.pone.0032435, 7(3): 1-12.

Rashmi, T. and B. Uyyanonvara, 2012. Curvature-based tortuosity evaluation for infant retinal images. J. Inform. Eng. Appl., 2(8): 9-18.

Robert, K., S.J. Teper, W. Beata, W. Edward, M.K. Micha and W. Zygmunt, 2012. Fully automatic algorithm for the analysis of vessels in the angiographic Image of the eye fundus. Biomed. Eng. Online, 11: 35.

Shankar, P.M., 1986. Speckle reduction in ultrasound B scans using weighted averaging in spatial compounding. IEEE T. Ultrason. Ferr., 33(6): 754-758.

Starck, J.L., F. Murtagh and A. Bijaoui, 1998. Image Processing and Data Analysis: The Multistage Approach. Cambridge University Press, Cambridge.

Starck, J.L. and F. Murtagh, 2001. Astronomical image and signal processing. IEEE Signal Proc. Mag., 18: 30-40.

Starck, J.L. and F. Murtagh, 2002. Astronomical Image and Data Analysis. Springer-Verlag, New York.

Starck J.L. and F. Murtagh, 2007. The undecorated wavelet decomposition and its reconstruction. IEEE T. Signal Proces., 16: 297-309.

Shaeb B.S and P.K. Satya, 2008. "Automatic Detection of Exudates in Diabetic Retinopathy Using Morphological Segmentation and Fuzzy Logic", IJCSNS International Journal of Computer Science and Network Security, 8(12): 211-218.

Vermeer, K.A., F.M. Vos, H.G. Lemij and A.M. Vossepoel, 2004. A model based method for retinal blood vessel detection. Comput. Biol. Med., 34: 209-219.

William, E.H., G. Michael, C. Brad, K. Paul and M.R. Nelson, 1999. Measurement and classification of retinal vascular tortuosity. Int. J. Med. Inform., 53: 239-252.

Wilson, C.M., K.D. Cocker, M.J. Moseley, C. Paterson, S.T. Clay, W.E. Schulenburg, M.D. Mills, A.L. Ells, K.H. Parker, G.E. Quinn, A.R. Fielder and J. Ng, 2008. Computerized analysis of retinal vessel width and tortuosity in premature infants. Invest Othalmol. Vis. Sci., 49: 3577-3585.

Wittchow, K., 2003. Shared Liability for ROP Screening. OMIC Journal.P.3 Retrieved from: http://www.omic.com/new/digest/DigestFall03.pdf.

Xiayu X., 2012. "Automated delineation and quantitative analysis of blood vessels in retinal fundus image", Ph.D. Thesis, University of Iowa.